Available online at www.sciencedirect.com
ScienceDirect
C. R. Mecanique 335 (2007) 336–341
COMPTES RENDUS MECANIQUE
http://france.elsevier.com/direct/CRAS2B/

Melting and solidification: processes and models/Experiments for solidification benchmarks

A quasi two-dimensional benchmark experiment for the solidification of a tin–lead binary alloy

Xiao Dong Wang, Patrick Petitpas, Christian Garnier, Jean-Pierre Paulin, Yves Fautrelle *

EPM/SIMAP/CNRS/INPG/ENSEEG Laboratory, B73, 38402 Saint Martin d'Hères cedex, France

Available online 21 June 2007

Abstract

A horizontal solidification benchmark experiment with pure tin and a binary alloy of Sn-10 wt.%Pb is proposed. The experiment consists in solidifying a rectangular sample using two lateral heat exchangers which allow the application a controlled horizontal temperature difference. An array of fifty thermocouples placed on the lateral wall permits the determination of the instantaneous temperature distribution. The cases with the temperature gradient $G = 0$, and the cooling rates equal to 0.02 and 0.04 K/s are studied. The time evolution of the interfacial total heat flux and the temperature field are recorded and analyzed. This allows us to evaluate heat transfer evolution due to natural convection, as well as its influence on the solidification macrostructure. ***To cite this article: X.D. Wang et al., C. R. Mecanique 335 (2007).***

Résumé

Expérience benchmark quasi-2D pour la solidification d'un alliage binaire étain–plomb. La présente étude consiste à analyser expérimentalement la solidification de l'étain pur et de l'alliage binaire d'étain Sn-10wt.%Pb. L'expérience consiste à solidifier un lingot parallélépipédique de faible épaisseur à l'aide de deux échangeurs latéraux qui permettent d'appliquer une différence de température entre les deux parois latérales et verticales. Un réseau de cinquante thermocouples placés sur la grande face latérale permet d'accéder à la distribution instantanée de la température. L'analyse post-mortem du lingot fournit la structure de solidification. Nous présentons les cas avec le gradient de température nul et des taux de refroidissement de 0,02 et 0,04 K/s respectivement. L'évolution temporelle du flux de chaleur et du champ de la température est mesurée et analysée. Ceci nous permet d'évaluer l'évolution de transfert thermique due à la convection normale, ainsi que son influence sur la macrostructure de solidification. ***Pour citer cet article : X.D. Wang et al., C. R. Mecanique 335 (2007).***

Keywords: Heat transfer; Solidification; Benchmark; Natural convection; Temperature field

Mots-clés : Transferts thermiques ; Solidification ; Benchmark ; Convection naturelle ; Champ température

1. Introduction

Natural or forced convection plays a very important role during solidification. Its intensity and flow pattern affect heat and mass transfer and, consequently, the solidification process, for example, macrostructure and segregation [1,2].

* Corresponding author.
E-mail addresses: xiaodong.wang@hmg.inpg.fr (X.D. Wang), yves.fautrelle@hmg.inpg.fr (Y. Fautrelle).

1631-0721/$ – see front matter
doi:10.1016/j.crme.2007.05.009

The latter effect has been shown by various experiments, and especially laboratory-scale solidification experiments, including the cases where electromagnetic fields have been imposed. However, the experimental results and conclusions could not easily be compared to each other because they have been performed with various the thermal boundary conditions [3–5]. This also renders difficult any comparison with numerical simulation results. The solidification process includes heat transfer, fluid flow, phase transition, segregation, and solute redistribution. Modelling of such complex phenomenon is a very difficult task. Experimental data for validation purposes are greatly needed. Thus, it is necessary to achieve a well-controlled experiment.

A quasi two-dimensional solidification experiment is proposed in the present work, whose aim is to build an experimental solidification benchmark and to provide useful quantitative data for the validation of numerical models. It is aimed at firstly recording in situ the heat transfer during the solidification of a parallelepipedic ingot and secondly at analyzing the corresponding post mortem solid structure and sample composition.

The temperature gradient is perpendicular to the gravitational field. Such a configuration promotes natural convection, which is known to influence the nature of the solidification (columnar or equiaxed structures appear) as well as the homogeneity of the solid, leading to the so-called macro-segregations. In the present article, we have focused our measurements on the temperature field and on structure analysis. Temperature measurements in a case where the cooling regime is symmetric on both sides of the sample are presented. In this article, the quasi two-dimension experimental model is presented and validated the next section; the experimental process is introduced in Section 3; the heat transfer and the solidification macro-segregation results are discussed in Section 4.

2. Description of the experimental model

The experiment set-up, as shown in Fig. 1, mainly consists of five parts: the sample of binary alloy Sn-10wt.%Pb, the stainless steel crucible with welded thermocouples and the temperature measurement system, the two lateral heat exchangers, the linear motor to generate a travelling magnetic field, the Kirchhoff box to control the radiative heat losses and the vacuum chamber to minimize natural convection around the sample.

In order to get a homogenous initial concentration, the pre-samples were melted in a quartz crucible by means of an induction device. Thanks to electromagnetic stirring, the various components were mixed after approximately 10 minutes. Then the melt was poured into a water-cooled copper crucible. The dimensions of the rectangular-shape sample are the following: its length is 10 cm, height 6 cm, and width 1 cm.

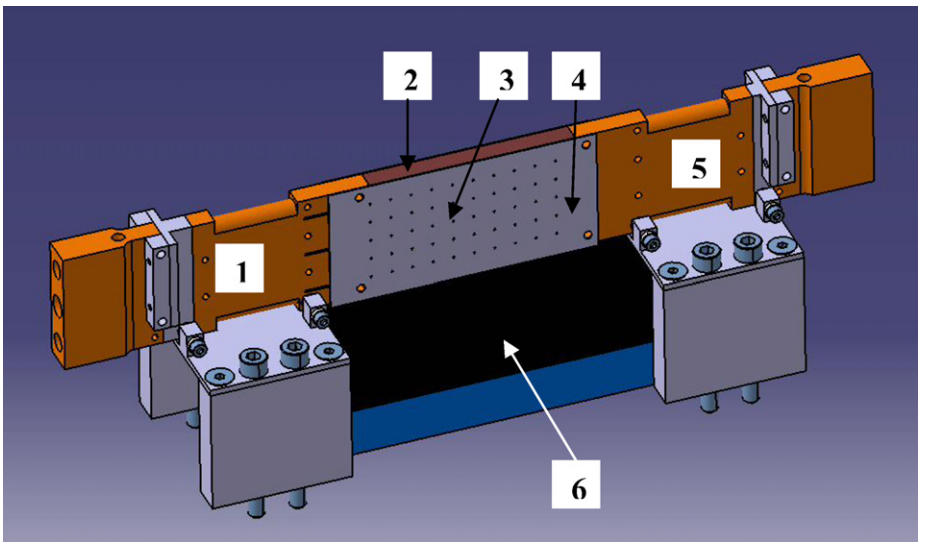

Fig. 1. Scheme of the experimental set-up: 1. Left heat exchanger, 2. Sn-10wt.%Pb sample, 3. Thermocouples position matrix, 4. The stainless steel crucible, 5. Right heat exchanger, 6. Linear motor.

Fig. 1. Le schéma de l'installation expérimentale. 1. Échangeur de chaleur gauche, 2. Échantillon de Sn-10wt.%Pb, 3. Réseau de thermocouples placé sur la face latérale du creuset, 4. Le creuset en acier inoxydable, 5. Échangeur de chaleur droit, 6. Moteur linéaire.

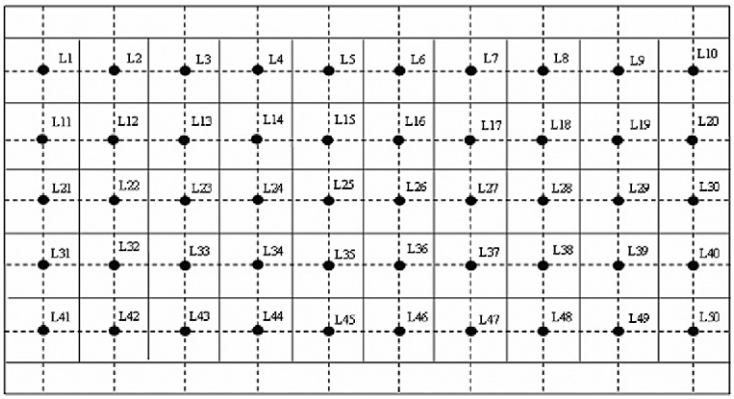

Fig. 2. The temperature measurement array on one of the largest surface of the crucible.

Fig. 2. La matrice de mesure de la température sur une des grandes faces du creuset.

A rectangular stainless steel crucible with a thin wall (thickness of 0.5 mm) is used. Meanwhile, the fifty type-K thermocouples were welded by means of a laser technique on one of its largest surfaces. The rectangular array of thermocouples allows the measurement of the instantaneous temperature field and its evolution during solidification. The distance between each thermocouple is 1 cm. The position and the reference of each thermocouple are shown in Fig. 2. All the temperatures are monitored and recorded numerically.

A copper heat exchanger was designed which employs the following characteristic: in the longitudinal direction, the cross-section approximately held the same shape as that in contact with the sample (1 cm × 6 cm). This may suppress the temperature difference due to the influence of the cross-section shape change. This point is very important to control precisely the heat transfer within the sample, as we desire. A part of stainless steel was used to slow the temperature drop. Six thermocouples are arranged in a three horizontal positions (each vertical distance is 2 cm) at each head of the heat exchanger to measure the heat flux at the interface, the horizontal distance between two thermocouples being $e_t = 1.5$ cm.

The main contribution to heat transfer between the crucible and its environment is radiation. A temperature-controlled Kirchhoff box, surrounding the sample, is used to compensate this radiation and to achieve adiabatic boundary conditions on the lateral walls. It comprises a temperature-regulated system including the cooling part and the electric heat resistance part. The radiative heat loss via the enclosure wall is estimated by the Stefan–Boltzmann law at less than 1.8 W. The heat transfer via convection and conduction are negligibly small since the sample is located in a vacuum chamber.

The top surface of the sample was covered with an insulating material which was sealed in aluminium film to decrease the heat transfer via radiation.

The low melt point pure tin and binary alloy of Sn-10wt.%Pb was used in this experimental work. This alloy belongs to the tin-base hypo-eutectic alloy family. The solidification range is 36.04 °C, ranging from the liquidus temperature equal to 219.46 °C to the eutectic, 183.42 °C. The extracted heat power ranges from 15 to 25 W depending on the metal type and the cooling rates. The heat lost by the stainless steel crucible is less than 1.4 W.

3. The experimental process

The temperatures are recorded at each second during the fusion and the solidification process. A series of thermocouples were imbedded in the head of the two heat exchangers to measure the heat flux extracted from the sample. Two of these thermocouples are placed at the center of the two contact surfaces between the exchangers and the sample in order to achieve a proper control of the temperature of the sample. They are called FR3 and FL3, for the right and left sides, respectively. The temperature difference between FR3 and FL3 divided by the length of the sample is defined as the imposed mean temperature gradient G. Note that this value does not represent the actual temperature gradient in the sample. The rate of temperature decrease of FR3 and FL3 are defined as the mean cooling rates. In this part, we study the situation where $G = 0$, and the mean cooling rates are $T' = 0.02$, 0.04 K/s. In order to maximize the thermal contact between the sample and the surface of the heat exchangers, we pre-melt it once. In the liquid zone,

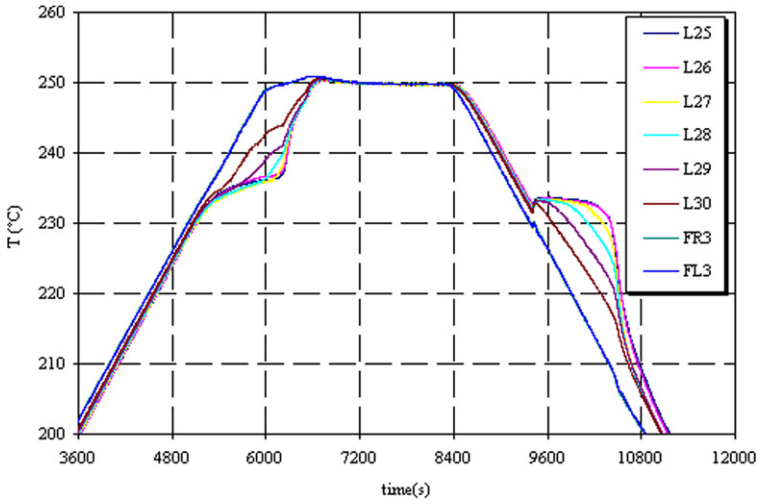

Fig. 3. Temperature-time evolution during the solidification of pure tin, $G = 0$, heating rate $\mathrm{d}T_f/\mathrm{d}t = 0.02$ K/s, cooling rate $\mathrm{d}T_s/\mathrm{d}t = -0.02$ K/s; FR3, FL3 are thermocouples measuring at the head of the heat exchangers, L26, L27, L28, L29, and L30 are the thermocouples whose positioning at the horizontal centerline are shown in Fig. 2.

Fig. 3. L'évolution temporelle de la température lors de la solidification de l'étain pur, $G = 0$, le taux de chauffage $\mathrm{d}T/\mathrm{d}t = 0,02$ K/s, le taux de refroidissement $\mathrm{d}T/\mathrm{d}t = -0,02$ K/s, les thermocouples FR3, FL3 sont situés à la tête des échangeurs de chaleur ; L26, L27, L28, L29, et L30 désignent les thermocouples dont l'emplacement le long de la ligne centrale horizontale est montré dans la Fig. 2.

electromagnetic stirring is used to homogenize the solute. Then one starts the experiment. According to the temperature regime, the profile can be divided into three steps. Fig. 3 shows the temperature–time evolution of the pure tin and the alloy of Sn-10wt.%Pb during the whole experiment process. The first step corresponds to the melting process; the temperatures of FR3 and FL3 are set to increase at a rate of 0.02 K/s to 250 °C, the sample melting being accomplished during this period. During the second step, the temperature is maintained, in order to get a relatively stable temperature field before the cooling step. During this step, the traveling magnetic field is imposed during 10 minutes in order to homogenize the bath. The third step is the solidification process during which the temperatures of FR3 and FL3 are set to decrease from 250 °C. Here we present two cooling rates: 0.02 and 0.04 K/s. Five temperature profiles measured by L26, L27, L28, L29, L30 (their positions are shown in Fig. 2) are shown in Fig. 3.

4. Experimental results and discussion

4.1. The temperature–time evolution

To clearly show the latent heat absorbing and releasing process, the solidification experiment with pure tin has been performed first. As the sample absorbs heat, its temperature increases; when the temperature reaches the tin melting point 231.9 °C, the sample would absorb the melt latent heat, while the temperature holds stable for a while. Because the heat transport comes from two sides, the melt heat release will be achieved from the two sides towards the centre; the temperature–time curves are shown as a bunch in Fig. 3. For pure tin, the plateau corresponding to the melting point of pure metal can be clearly seen in Fig. 3. However, for the alloy of Sn-10wt.%Pb, the latent heat absorption or extraction process is visible in the temperature–time evolution curve.

4.2. Temperature field evolution

The measurement error of the temperature field comes from two aspects: on the one hand, intrinsic error of the thermocouples, and on the other hand, the uncontrolled heat losses from set-up itself, i.e. the lateral surface of the sample which is not ideally thermally insulated and uniform. To assess the importance of these two types of error, we held the temperature of the liquid bulk of pure tin at 250 °C for 700 s, the temperature difference varied randomly in the range of 0.3 °C. Then the entire temperature field is calibrated with this data.

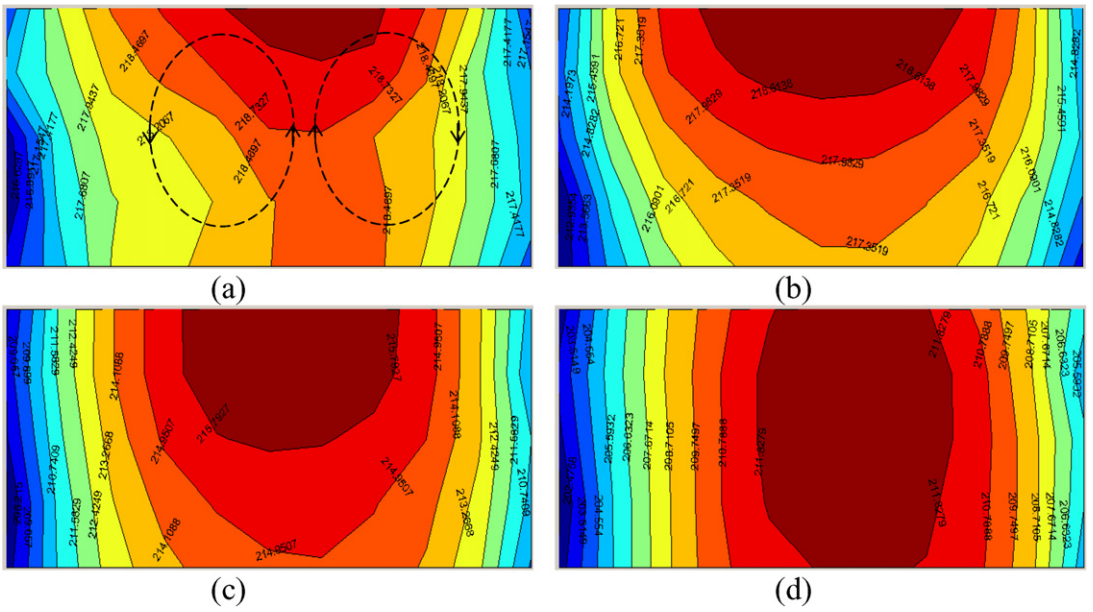

Fig. 4. Recorded instantaneous temperature field maps during solidification of a Sn-10wt.%Pb alloy. $G = 0$, $\mathrm{d}T/\mathrm{d}t = 0.02$ K/s. (a) $t = 9500$ s, (b) $t = 9800$ s, (c), $t = 10\,100$ s, (d) $t = 10\,400$ s.

Fig. 4. Enregistrement du champ de la température instantané pendant la solidification de l'alliage Sn-10wt.%Pb. $G = 0$, $\mathrm{d}T/\mathrm{d}t = 0{,}02$ K/s. (a) $t = 9500$ s, (b) $t = 9800$ s, (c), $t = 10\,100$ s, (d) $t = 10\,400$ s.

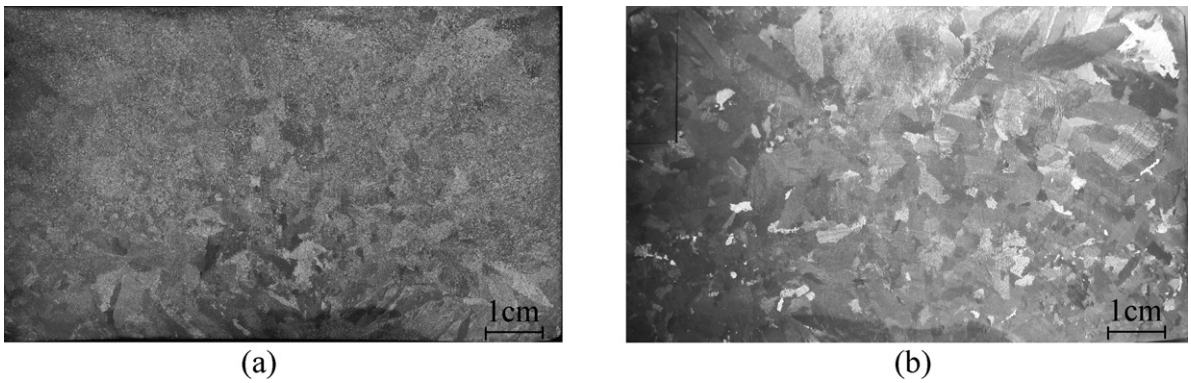

Fig. 5. Solidification macrostructure of Sn-10wt.%Pb alloy at the different mean cooling rates: (a) $\mathrm{d}T_1/\mathrm{d}t = 0.02$ K/s, (b) $\mathrm{d}T_2/\mathrm{d}t = 0.04$ K/s, $G = 0$.

Fig. 5. Macrostructure de solidification d'alliage de Sn-10wt.%Pb pour deux taux de refroidissement moyen différents : (a) $\mathrm{d}T/\mathrm{d}t = 0{,}02$ K/s, (b) $\mathrm{d}T/\mathrm{d}t = 0{,}04$ K/s, $G = 0$.

Due to the existence of thermo-solutal convection in the mushy zone, the alloy of Sn-10wt.%Pb behaves in a different manner compared with the pure tin. It is of interest to consider the temperature distribution and evolution in the mushy zone in the case of the Sn-10wt.%Pb alloy. Fig. 4 shows the temperature field with the cooling rate $\mathrm{d}T/\mathrm{d}t = 0.02$ K/s at four moments, i.e., $t = 9500$, 9800, 10 100 and 10 400 s. As shown in Fig. 4(a), the flow pattern schematically consists of two circulations, the arrows showing the flow's probable directions. It can be seen that in the upper side of the centre part, a region (fully liquid or mushy zone) with almost uniform temperature occurred, as seen in Figs. 4(a)–(c). This is the likely effect of the natural convection. Indeed, at the end of the solidification in Fig. 4(d) the isotherms become almost vertical as in a solid cooled from both sides. The temperature difference at each map increases as the time increases. The maximum value can reach nearly 10 K.

4.3. Observation of the grain structure

Fig. 5 shows the grain structure for the different cooling rates. As shown in Fig. 5(a), a large region of equiaxed can be found; we expect a small columnar region near the bottom in the center part. This may be explained by the fact that the macrostructure is affected by the flow pattern along the solidification front. The columnar dendrites exposed to fluid flow change their direction of growth to grow into the upstream direction of the flow, the flow trend being illustrated in Fig. 4(a). When the cooling rate was increase to 0.04 K/s, the columnar zone is larger than that obtained in the previous case, as showed in Fig. 5(b). Many long columnar grains are formed at the two sides near the upper part of the sample, where there may exist a larger temperature gradient.

In summary, a quasi two-dimensional experimental benchmark model, aimed at studying the solidification process, natural convective flow, and temperature distribution, has been performed. The experiment has proved its ability to achieve a well-controlled solidification.

Acknowledgements

The authors would like to acknowledge financial support provided by ESA (Europe Space Agency) under the project CETSOL (Columnar-to-Equiaxed Transition of Solidification).

References

[1] Y. Fautrelle, Solidification of metallic alloys under the influence of various types of AC magnetic field, Keynote lecture, in: ASIAN EPM 2005, 2nd Asian Workshop on Electromagnetic Processing of Materials, Shenyang, RP China, May 2005, pp. 22–25.

[2] X.D. Wang, A. Ciobanas, F. Baltaretu, A.M. Bianchi, Y. Fautrelle, Control of the macrosegregation during solidification of a binary alloy by means of AC magnetic field, in: 4th Int. Conf. on Solidification and Gravity, Miskolc, 6–10 September 2004, ed. by Transtech.

[3] D.J. Hebditch, J.D. Hunt, Observations of ingot macrosegregation on model systems, Metallurgical Trans. 5 (July 1974) 1557–1563.

[4] C.A. Siqueira, N. Cheung, A. Garcia, The columnar to equiaxed transition during solidification of Sn–Pb alloys, J. Alloys Compounds 351 (2003) 126–134.

[5] L.H. Shaw, J. Beech, R.H. Hickley, Channel segregates in cast steel rolls, Ironmaking Steelmaking 13 (1986) 154–160.